Article

SOURCE DATA | TRANSPARENT PROCESS

THE EMBO JOURNAL

Hierarchical protein targeting and secretion is controlled by an affinity switch in the type III secretion system of enteropathogenic *Escherichia coli*

Athina G Portaliou[1], Konstantinos C Tsolis[1], Maria S Loos[1], Vassileia Balabanidou[2], Josep Rayo[1], Alexandra Tsirigotaki[1], Valerie F Crepin[3], Gad Frankel[3], Charalampos G Kalodimos[4], Spyridoula Karamanou[1,*] & Anastassios Economou[1,**]

Abstract

Type III secretion (T3S), a protein export pathway common to Gram-negative pathogens, comprises a trans-envelope syringe, the injectisome, with a cytoplasm-facing translocase channel. Exported substrates are chaperone-delivered to the translocase, EscV in enteropathogenic *Escherichia coli,* and cross it in strict hierarchical manner, for example, first "translocators", then "effectors". We dissected T3S substrate targeting and hierarchical switching by reconstituting them *in vitro* using inverted inner membrane vesicles. EscV recruits and conformationally activates the tightly membrane-associated pseudo-effector SepL and its chaperone SepD. This renders SepL a high-affinity receptor for translocator/chaperone pairs, recognizing specific chaperone signals. In a second, SepD-coupled step, translocators docked on SepL become secreted. During translocator secretion, SepL/SepD suppress effector/chaperone binding to EscV and prevent premature effector secretion. Disengagement of the SepL/SepD switch directs EscV to dedicated effector export. These findings advance molecular understanding of T3S and reveal a novel mechanism for hierarchical trafficking regulation in protein secretion channels.

Keywords chaperone; EPEC; *in vitro* reconstitution; substrate switching; type III secretion

Subject Categories Membrane & Intracellular Transport; Microbiology, Virology & Host Pathogen Interaction

DOI 10.15252/embj.201797515 | Received 6 June 2017 | Revised 5 September 2017 | Accepted 11 October 2017 | Published online 6 November 2017

The EMBO Journal (2017) 36: 3517–3531

Introduction

Several Gram-negative pathogens use the type III protein secretion system (T3SS) to inject virulence proteins directly into eukaryotic host cytoplasms (Portaliou *et al*, 2016; Deng *et al*, 2017). T3SS comprises the "injectisome", a complex, bacterial envelope-associated, syringe-like organelle, with four parts: (i) a membrane-embedded translocase (or export apparatus) that associates with peripheral inner membrane structures including an ATPase. (ii) the basal body, comprising stacked rings spanning both bacterial membranes, connected by an inner rod, which transverses the periplasm. (iii) a protruding needle and (iv) the "translocon"; located at the tip of the needle to form a pore in the host plasma membrane through which bacterial toxins are injected.

T3SS-exported proteins contain non-homologous N-terminal signal sequences (Deng *et al*, 2015) and are maintained in secretion-competent states by cytoplasmic chaperones (Parsot, 2003; Wilharm *et al*, 2007). Chaperones are small, frequently dimeric, and fall in five classes; for example, class V binds early export substrates like the rod and needle subunits; class III and class IV preferentially bind middle substrates like translocators; I, interacts with late effectors.

A unique characteristic of T3S is that secretion through the translocase occurs in consecutive steps of defined, strict hierarchy, secured by poorly understood switching mechanisms that include gatekeeper proteins like SepL of EPEC (Portaliou *et al*, 2016; Deng *et al*, 2017). Gatekeepers carry their own secretion signals and class I heterodimeric chaperone suggesting they might act like pseudo-effectors (Schubot *et al*, 2005; Botteaux *et al*, 2009; Burkinshaw *et al*, 2015).

To dissect the molecular mechanism of substrate targeting and switching during T3S, we used enteropathogenic *Escherichia coli*

1 Laboratory of Molecular Bacteriology, Department of Microbiology and Immunology, Rega Institute for Medical Research, KU Leuven, Leuven, Belgium
2 Institute of Molecular Biology and Biotechnology, FORTH (Foundation of Research and Technology), University of Crete, Heraklion, Greece
3 Department of Life Sciences, MRC Centre for Molecular Bacteriology and Infection, Imperial College London, London, UK
4 University of Minnesota, Biochemistry, Molecular Biology & Biophysics, Minneapolis MN, USA
*Corresponding author. Tel: +32 16 379208; E-mail: lily.karamanou@kuleuven.be
**Corresponding author. Tel: +32 16 379273; Fax: +32 16 330026; E-mail: tassos.economou@kuleuven.be

(EPEC) that attach to host cells, disrupt microvilli, cause actin rearrangements and infantile diarrhea (Dean & Kenny, 2009). Our model translocator exported protein EspA forms an outer needle sheath (Knutton *et al*, 1998) and is stabilized for export by CesAB, a 3-helix, dimeric chaperone (Fig 1A; Creasey *et al*, 2003; Yip *et al*, 2005; Chen *et al*, 2011). Two helices from both EspA-termini bind through coiled-coil interactions with CesAB and monomerize it (Yip *et al*, 2005). EspA, although structurally distinct, shares sequence homology and presumably functions with needle tip proteins from other T3SS (Sato & Frank, 2011; Portaliou *et al*, 2016; Deng *et al*, 2017). Our model effector protein is Tir (translocated intimin receptor), chaperoned by CesT (Abe *et al*, 1999; Thomas *et al*, 2005).

We have now reconstituted T3SS targeting *in vitro*, using inverted inner membrane vesicles (IMVs) from EPEC, and revealed a novel mechanism that, on the one hand, governs translocator targeting and secretion and on the other the switching to effector export. While the "N-core" of CesAB (aa 1–86) contains the EspA chaperoning function, its unstructured "C-tail" is a previously unknown translocase targeting signal. High-affinity CesAB docking occurs on a bipartite receptor that comprises the gatekeeper SepL (O'Connell *et al*, 2004), which associates tightly with the membrane and the C-terminal domain of EscV, a membrane-embedded subunit of the translocase (Gauthier *et al*, 2003; Abrusci *et al*, 2013). Binding of SepL on EscV reduces the affinity of chaperone/effector complexes, such as CesT/Tir, for EscV. SepL removal allows enhanced Tir affinity and secretion. Thus, SepL acts as a substrate affinity switch. SepD, one of the SepL chaperones (Deng *et al*, 2005), modulates the SepL-EscV interaction, presumably by altering the conformation of SepL. SepD together with the CesAB C-tail couple the receptor function of SepL to translocator secretion. Our findings provide quantitative molecular understanding of the T3S targeting process, a novel mechanism for regulating protein trafficking channels and set the stage for the complete mechanistic and biophysical dissection of the T3S machine.

Results

CesAB comprises two structurally and functionally distinct domains

To define chaperone and targeting elements in CesAB, we first analyzed its domain organization and flexibility (Fig 1A) by using hydrogen deuterium exchange mass spectrometry [HDX-MS (Tsirigotaki *et al*, 2017b) (Fig 1B; Appendix Table S1)]. The N-core is stabilized by either EspA binding (Fig 1B, middle) or mimicking mutations (right; i.e., CesAB(D14L/R18D/E20L), hereafter DRE (Chen *et al*, 2013). In contrast, the C-tail remains unstructured in all cases (Fig 1B; Appendix Table S1). Limited trypsinolysis corroborated these results (Fig EV1A).

Like CesAB, CesAB(ΔC) (Fig 1A), a C-tail truncate, is dimeric and forms 1:1 stoichiometric complexes with EspA *in vitro* (Fig EV1B) and *in vivo* (Fig EV1C–F). Six basic C-tail residues are responsible for CesAB's pI of 9.5 (Fig EV1G).

In summary, CesAB comprises the self-dimerizing, EspA binding, N-core (Yip *et al*, 2005; Chen *et al*, 2011) and an unstructured, positively charged C-tail.

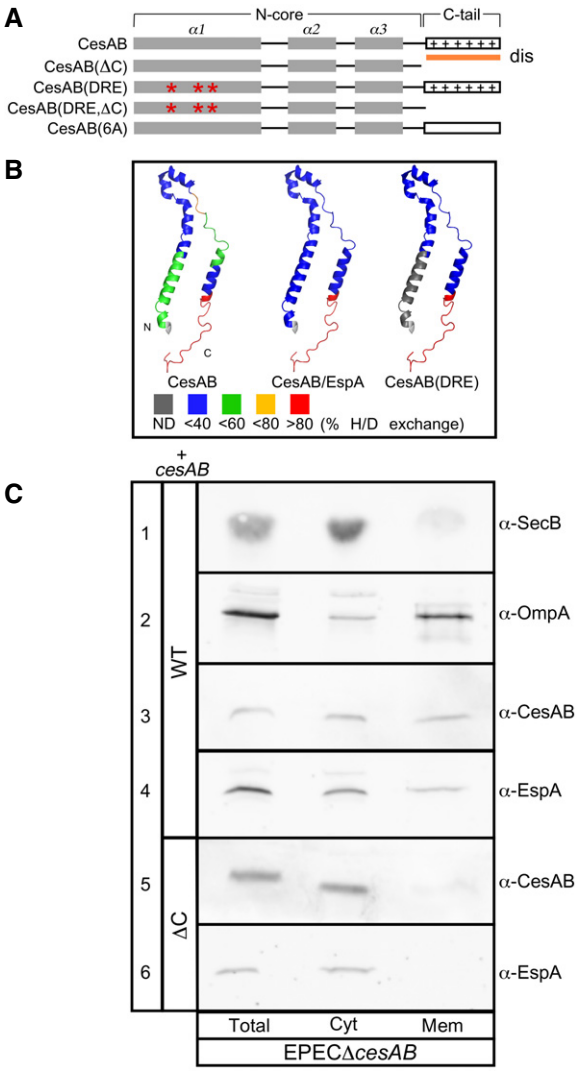

Figure 1. CesAB comprises two structural and functional distinct domains.

A Schematic representation of CesAB. The N-core (α1–3 helices), C-tail (aa: 86–107 that remain unresolved), and mutated derivatives are indicated. Dis, disorder prediction; *, mutations; +, positive charges R89, K91, R99, R101, R104, and K105.

B Local HDX-MS analysis of CesAB, CesAB(DRE), and CesAB/EspA, mapped on a CesAB protomer. Cold colors: rigid regions (e.g., N-core); hot colors: unstructured, solvent-accessible, non-hydrogen-bonded regions (e.g., the C-tail). ND: not determined. See Appendix Table S1 for peptides.

C Sub-cellular localization of CesAB and EspA in EPECΔ*cesAB* cells expressing plasmid-borne *cesAB* or *cesAB*(ΔC) (see also Fig EV2A). Following fractionation, equal fraction volume (Total, cell proteins; Cyt, cytoplasmic; Mem, membrane) was analyzed on 15% SDS–PAGE and immunostained. Lane 1: cytoplasmic protein SecB; lane 2: membrane protein OmpA. $n = 3$.

Source data are available online for this figure.

C-tail-dependent CesAB/EspA targeting to the membrane

To determine whether CesAB/EspA are targeted to the membrane, EPECΔ*cesAB* cells expressing *cesAB in trans* were lysed, cytoplasmic and membrane fractions were separated by centrifugation, and polypeptides analyzed on SDS–PAGE and immunostained (Fig 1C).

Fractionation efficiency was monitored by following a cytoplasmic (row 1; SecB) and an outer membrane (row 2; OmpA) protein. CesAB (row 3) and EspA (row 4) were detected in both fractions. In contrast, both proteins were found exclusively in the cytosol of EPECΔ*cesAB* carrying a *cesAB(ΔC)* plasmid (Fig 1C, rows 5 and 6). Membrane-bound CesAB associated peripherally since high ionic strength or urea removed it, unlike EspA that remained membrane-associated (Fig EV2A).

We concluded that (i) CesAB is targeted to the membrane, (ii) targeting requires the C-tail, (iii) EspA is co-targeted, and (iv) once there, EspA remains membrane-associated independently of CesAB.

In vitro reconstitution of CesAB/EspA targeting

To determine its specificity for the T3S translocase and further dissect it, we reconstituted CesAB/EspA targeting *in vitro*. IMVs prepared from EPEC cells were urea-treated, to strip away most of the peripheral and non-specifically associated proteins (Papanastasiou *et al*, 2016; Tsolis & Economou, 2017a). The external side of the IMVs is the one that faced the cytoplasm in the cell; their lumen represents the periplasmic face. We demonstrated that EPEC-derived IMVs were functionally similar to those prepared from the non-EPEC strain BL31, using two functional assays derived from the ubiquitous Sec system (Gouridis *et al*, 2010): the proPhoA-stimulated Sec translocase ATPase and proPhoA translocation in the lumen of the IMVs (Fig 2A and B).

Mass spectrometric (MS) analysis of surface-accessible proteins from EPEC IMVs (Papanastasiou *et al*, 2013; Tsolis & Economou, 2017a) prior and post-urea treatment confirmed the presence of the injectisome by identifying several integral membrane components (e.g., EscV, EscD, EscJ, Fig 2C, and EscU; Fig EV2B; Appendix Table S2). Immuno-gold electron microscopy using an antibody against the cytoplasmic EscV C-domain confirmed that it is surface-exposed in EPEC IMVs. No non-specific labeling was seen on BL31 IMVs (Fig EV2C). As expected, the chaotrope removed most of the T3SS proteins that are peripherally associated on IMVs, but not the integral membrane components (Fig 2C), except EscU, whose C-terminal domain becomes cleaved and removable (Appendix Table S2).

We next used urea-treated IMVs in a flotation assay (Karamanou *et al*, 2008). BL31 (Fig 2D, rows 1–3) or EPEC (rows 6–9) IMVs, loaded at the bottom of a sucrose gradient, floated up, to their corresponding density, during ultracentrifugation. Migration inside the gradient was monitored by immunostaining of an inner membrane protein (rows 1 and 6; SecY). The peripheral membrane protein SecA that binds to SecY (Tsirigotaki *et al*, 2017a) floated up in the presence of IMVs, co-migrating with them (rows 2 and 7), but remained at the bottom in their absence (row 4). Under the same conditions, CesAB/EspA floated up to the top fractions in the presence of EPEC IMVs (rows 8 and 9; quantification of 9 is shown below the row) but remained at the bottom of the gradient in their absence (row 5) or in the presence of BL31 IMVs (row 3). These results demonstrated that CesAB/EspA bind specifically to a receptor on EPEC-derived IMVs, presumably the injectisome, and do not bind non-specifically to lipids or generic *E. coli* membrane components shared with BL31.

Next, we determined the equilibrium dissociation constants (K_d) of CesAB/EspA for EPEC and BL31 IMVs, by concentration titrations of [^{35}S]-CesAB/EspA, using protocols routinely used for the Sec system (Gouridis *et al*, 2010, 2013). CesAB/EspA bind with high affinity ($K_d \sim 0.16$ μM) to a saturable receptor on EPEC IMVs but only non-specifically, non-saturably to BL31 IMVs (Figs 2E and EV2D, top).

These data demonstrated successful reconstitution of targeting of T3S chaperone/exported proteins *in vitro* using EPEC-derived IMVs.

CesAB/EspA targeting to the injectisome requires SepL and EscV

We hypothesized that the CesAB/EspA receptor comprises injectisome components that reside on the cytoplasmic face of the membrane and that would be surface-exposed on the IMVs (Fig 3A, dark gray). To identify them, we generated whole and partial (i.e., encoding the large cytoplasmic domains of *escV* and *escU*) chromosomal gene deletions. None of the derivative strains secreted EspA *in vivo* (Fig 3B; Appendix Fig S1A), in agreement with previous results (Dziva *et al*, 2004; O'Connell *et al*, 2004; Nadler *et al*, 2006; Deng *et al*, 2015), nor formed actin pedestals on HeLa cells (Appendix Fig S1D–L), an assay reporting effector injection (e.g., Tir) *via* the EspA filaments and the EspB/D translocon pore (Creasey *et al*, 2003).

We next prepared urea-treated IMVs from all the deletion strains and quantified CesAB/EspA targeting to them using flotation assays (Fig 3C; Appendix Fig S1B). Chromosomal deletions of *cesAB*, *sepD*, *escN*, *escQ, and escU*(Δ*CD*) did not or only moderately affect(ed) CesAB/EspA targeting to the injectisome (Fig 3C, rows 2, 3, 6, 7, and 8, respectively). On the contrary, CesAB/EspA did not bind to IMVs devoid of SepL, CesL, or the C-domain of EscV (rows 4, 5, and 9). Since only some EPEC deletion strains were targeting-deficient (compare Fig 3C to B), targeting can be biochemically dissected from downstream secretion steps.

Quantification of the SepL content of IMVs, by immunostaining (Fig 3D; Appendix Fig S1C), pointed out that three IMV preparations that were deficient in CesAB/EspA targeting (Fig 3C, rows 4, 5 and 9), also had low SepL levels (Fig 3D, rows 4, 5 and 9). CesL, a SepL chaperone (Younis *et al*, 2010), might stabilize SepL. EscU and EscQ appear also to contribute to SepL accumulation at the membrane and may have non-essential regulatory roles in CesAB/EspA binding. The role of these proteins was not pursued further. Hereafter, we focused on SepL and EscV as potential CesAB/EspA receptor components.

SepL tightly associates with the membrane *via* its N-terminus

Unlike the membrane-embedded EscV, SepL has properties of a soluble protein, with a disordered N-terminus (Fig 3E) and no extensive hydrophobic patches (Burkinshaw *et al*, 2015). Yet, a chaotrope (8 M urea) could only poorly extract SepL from the membrane; complete extraction required increasing concentration of non-ionic detergent (Figs 3F and EV3A), suggesting a tight SepL–membrane association. While the N-terminus of SepL is trypsin-accessible in solution (Fig 3G, lanes 3–6), cleaved at R73 (Fig 3E), it becomes trypsin-resistant upon membrane association (Fig 3G, lanes 7–9) suggesting SepL association with the membrane *via* its N-terminus. Corroborating this, three C-terminal truncated or mutated derivatives remained membrane-bound (Fig EV3B). Membrane-associated SepL is fully trypsinized after longer incubation (Fig 3G, lanes 10–12) and therefore fully exposed and peripheral.

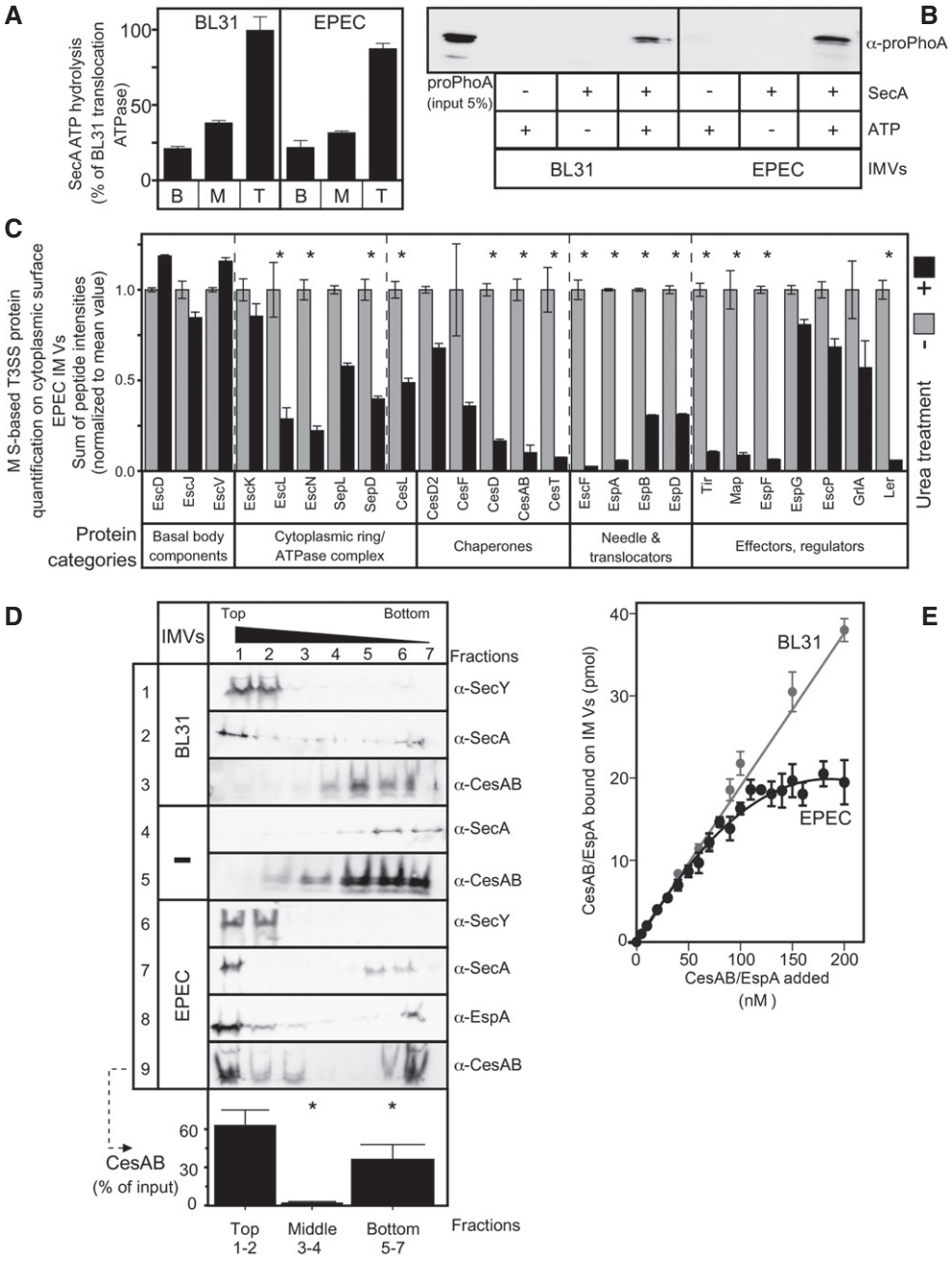

Figure 2. ***In vitro*** **reconstitution of type III chaperone/exported protein targeting.**

A, B Urea-treated IMVs prepared from BL31 (left) and wild-type EPEC (right) strain retained similar enzymatic properties, that is, stimulation of SecA ATP hydrolysis (B, basal; M, membrane; T, translocation ATPase) (A) and proPhoA translocation into the lumen of IMVs, *in vitro* (B). $n = 5$; bar graphs represent mean values; error bars standard deviation (SD).

C Bottom-up, liquid chromatography-mass spectrometry-based analysis of T3SS components on IMVs prior (light gray) or post (dark gray)-urea treatment. The relative abundance of components (sum of peptide intensities) for the multiple repeats tested, from various T3SS proteins, grouped by function, is shown in bar graphs with error bars (standard error of the mean); $n = 5$. Differentially abundant proteins with P-value < 0.05, as determined by t-test and adjusted by BH and fold change > 2 (see Materials and Methods) are indicated with an asterisk (*). See Appendix Table S2 for details.

D CesAB/EspA binding to urea-treated EPEC IMVs, using a flotation assay. Fractions were analyzed by 15% SDS–PAGE and immunostaining. SecY, membrane-embedded protein; SecA, cytoplasmic protein that binds SecY, which are shown as controls. Soluble proteins remained at the bottom (fractions 5–7) or co-migrated with IMVs once bound on them at the top of the gradient (fractions 1 and 2). The CesAB signal quantification (from row 9) is shown as % of the input, below the row. $n = 6$; bar graphs represent mean values; error bars standard deviation (SD). Significant difference with P-values < 0.05, as determined by t-test and adjusted by BH (see Materials and Methods) is indicated with an asterisk (*).

E Determination of equilibrium dissociation constants (K_d) of CesAB/EspA for EPEC (black) and BL31 (gray) IMVs. Data, analyzed by nonlinear regression, represent average values; error bars, standard mean error (SEM). BL31 IMVs exhibited linear, non-saturable binding, which did not converge to a K_d. $n = 9$–12.

Source data are available online for this figure.

SepL physically interacts with the C-domain of EscV

The absence of SepL from EPEC*escV(ΔCD)* IMVs (Fig 3D, row 9) suggested that the EscV C-domain might be a binding scaffold for SepL. To determine whether the two interact, we probed arrays of immobilized SepL peptides (13-mers; 10 residue overlaps) with the EscV C-domain (Fig EV4A, B, and E). Interacting residues localized primarily on two sites (d and e) on one face of SepL, in domains 2 and 3 (Fig 3H, red). In the reciprocal experiment, EscV C-domain peptide arrays were probed with SepL (Fig EV4C, D, and F). When

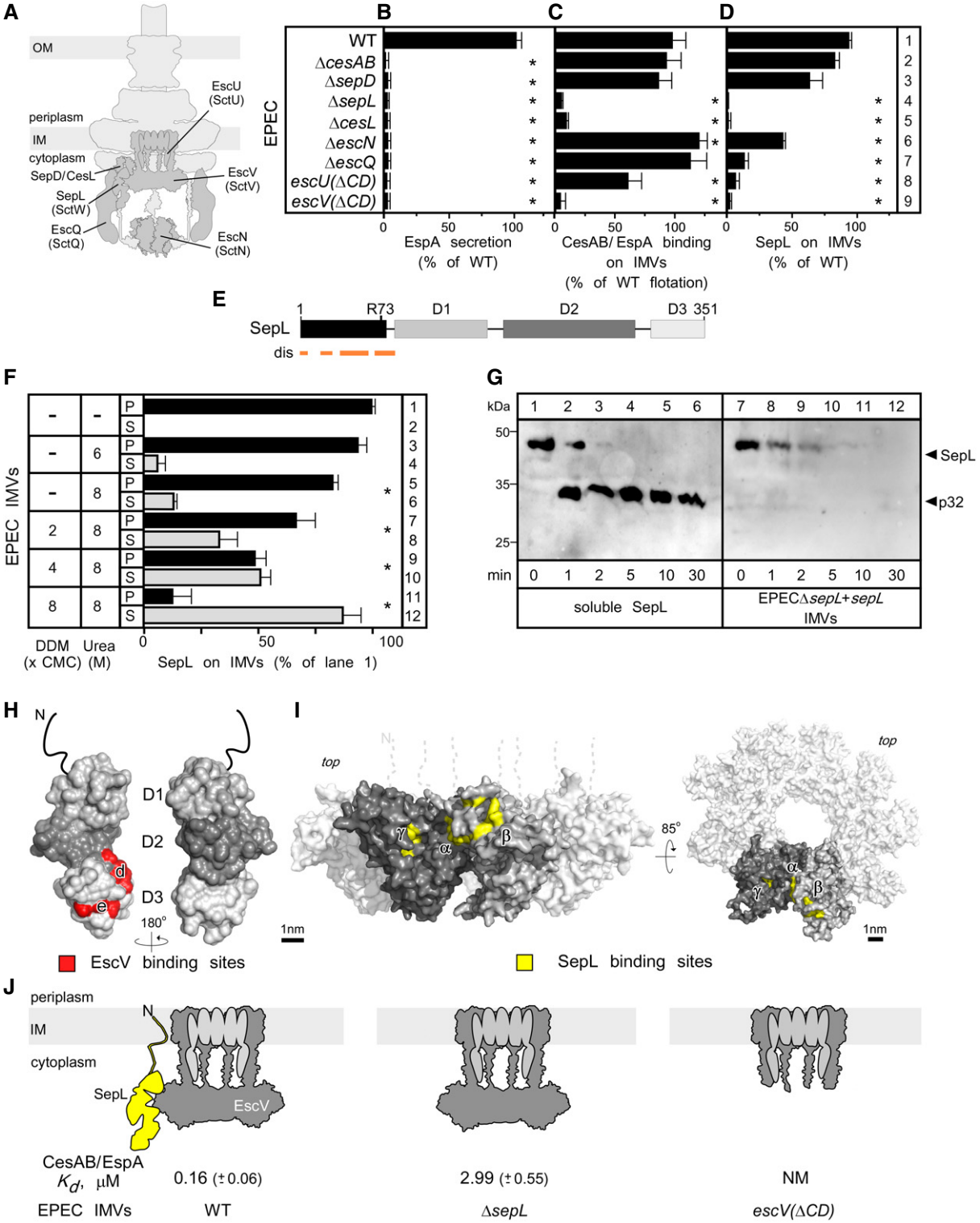

Figure 3.

the linear peptide signals were mapped on the EscV monomer structure model derived from the structure of the *Shigella* homologue (Abrusci *et al*, 2013), it was revealed that SepL bound to three external surfaces. When mapped on the nonamer ring model, they could form a groove between two neighboring protomers containing two adjacent binding sites (α and β) on one protomer and site γ on its neighbor (Fig 3I, yellow; Fig EV4F). We concluded that SepL physically interacts with the C-domain of EscV.

SepL and EscV form a bipartite CesAB/EspA receptor

To quantify the contributions of SepL and EscV as CesAB/EspA receptor components, we compared the equilibrium dissociation constants (K_ds) of CesAB/EspA for IMVs prepared from wild-type EPEC, EPEC*ΔsepL*, and EPEC*escv(ΔCD)* cells (Figs 3J and EV2D). Only when both SepL and EscV were present (Fig 3J, left), CesAB/EspA was targeted to the injectisome with high affinity (0.16 μM). When SepL was absent but EscV present (middle), CesAB/EspA exhibited only low affinity for the injectisome (~3 μM). When the EscV C-domain was deleted (right), SepL did not associate with the membrane and the affinity of CesAB/EspA for the injectisome was non-measurable.

We concluded that SepL and EscV form a bipartite receptor. SepL, apparently operates like an accessory injectisome subunit, associates with the membrane and with the C-domain of EscV (Fig 3J, left), thus securing high-affinity CesAB/EspA targeting to the injectisome.

CesAB/EspA binding sites on SepL are essential for its receptor function

Chemical cross-linking of CesAB to soluble (Fig EV3D, lanes 3 and 6) or IMV-associated SepL (Fig EV3E, lanes 2 and 6) suggested a direct interaction of CesAB/EspA with SepL. To identify the interaction sites, the SepL peptide array was incubated with CesAB/EspA, or CesAB, or their derivatives (Fig EV4A, B, and E). Three CesAB N-core-specific binding sites were identified on one face of SepL, in domains 1 and 3 (Fig 4A, left, green and B). Two of these sites ("a" and "e") are composite, comprising residues that are distant in the primary but come together in the 3D structure. Some residues overlapped with the EscV C-domain binding sites of SepL (Figs 3H and EV4A and E). The positively charged CesAB C-tail seemed to recognize two negatively charged sites (b; c) on the other face of SepL (Fig 4A, right, green and B).

To test the importance of these associations, the implicated surface-exposed SepL residues (Fig 4A) were alanyl or seryl substituted on plasmid-borne *sepL* (Fig EV4E; detailed in Appendix Supplementary Materials and Methods). We transformed these plasmids in EPEC*ΔsepL* cells, prepared IMVs, and determined their SepL content and affinity for CesAB/EspA. All mutants retained the membrane association of SepL (Fig 4C; Appendix Fig S2A) but had lost high-affinity CesAB/EspA binding (Fig 4D, compare rows 3–7 to 2).

Our results demonstrated that CesAB/EspA physically associated with specific SepL sites that are essential for its high-affinity binding to the translocase. Peptide arrays provide neither temporal order nor stoichiometries.

High-affinity CesAB binding to SepL requires the CesAB C-tail

Do both CesAB and EspA bind on SepL? Since EspA aggregates in the absence of its chaperone [Fig EV1D, E and F, compare lanes 2 and 3 to lane 1 (Creasey *et al*, 2003)], we could only probe this question using CesAB/EspA, or CesAB alone, or their derivatives.

CesAB alone had low affinity for the translocase (Fig 4E, 2.5 μM). Only when loaded with EspA in a 1:1 heterodimer, CesAB acquired its high-affinity binding conformation (0.16 μM). CesAB (DRE), a mutant that mimics this conformation (Chen *et al*, 2013), bound with high affinity on wild-type EPEC IMVs (0.39 μM) and

Figure 3. SepL and EscV form a bipartite CesAB/EspA receptor.

A Schematic representation of the T3S injectisome (Portaliou *et al*, 2016). Subunits analyzed here are in dark gray; Esc, EPEC-specific; Sct, universal names. Based on their homology with *Yersinia* (Schubot *et al*, 2005), SepD and CesL might form a heterodimer at the membrane.

B The EspA secretion from various EPEC knockout strains (5 h post-inoculation; Appendix Fig S1A) was quantified. WT secretion was considered 100%; all other values are expressed as % of this. $n = 3$; bar graphs represent mean values; error bars standard deviation (SD). Significant difference with P-values < 0.05, as determined by t-test and adjusted by BH (see Materials and Methods) is indicated with an asterisk (*).

C CesAB/EspA binding to urea-treated IMVs, from various EPEC knockout strains, on flotation assays (Appendix Fig S1B) was quantified (as in lane 9, Fig 2D). The CesAB amount that migrated in the top gradient fraction upon incubation with wild-type EPEC IMVs was considered 100%; all other values are expressed as % of this; $n = 5$; bar graphs represent mean values; error bars standard deviation (SD). Significant difference with P-values < 0.05, as determined by t-test and adjusted by BH (see Materials and Methods) is indicated with an asterisk (*).

D SepL content on IMVs. Following analysis of equal protein amount from various urea-treated EPEC IMVs on 15% SDS–PAGE and immunostaining (Appendix Fig S1C), signals were quantified. SepL amount on wild-type IMVs was considered 100%; all other values are expressed as % of this. $n = 3$; bar graphs represent mean values; error bars standard deviation (SD). Significant difference with P-values < 0.05, as determined by t-test and adjusted by BH (see Materials and Methods) is indicated with an asterisk (*).

E A linear map of SepL, indicating D1–3 domains, disordered predicted regions (dis) and the trypsin cleavage site in solution (R73).

F The association of SepL with the membrane is tight. EPEC IMVs (40 μg protein) were treated with the indicated urea or/and dodecyl maltoside (DDM) concentration (30 min; ice), ultracentrifuged (100,000 *g*, 30 min, 4°C; TLA100 rotor; Optima Max-XP Beckman), analyzed on 15% SDS–PAGE, and immunostained (Fig EV3A). Signals were quantified. The SepL amount of untreated IMVs (lane 1) was considered 100%; all other values are expressed as % of this. S: supernatant; P: pellet; error bars represent the standard deviation. $n = 4$. Significant difference with P-values < 0.05, as determined by t-test and adjusted by BH (see Materials and Methods) is indicated with an asterisk (*).

G Limited trypsinolysis of SepL, in solution (lanes 1–6) or bound on IMVs (lanes 7–12), after immunostaining with α-SepL (as in Fig EV1A); $n = 6$.

H On the surface structure of SepL (PDB accession number: 5C9E), the EscV C-domain binding sites, as determined by peptide array analysis (Fig EV4A and B), are shown (red; Latin letters).

I On two adjacent protomers (dark and light gray) of the nonameric EscV surface model [derived from the *Shigella* homologue, MxiA (Abrusci *et al*, 2013)], the SepL-binding sites, as determined by peptide array analysis (Fig EV4C and D), are shown (yellow; Greek letters).

J CesAB/EspA targeting to the T3S translocase in wild-type, Δ*sepL* and *escV(ΔCD)* IMVs; $n = 6$; mean ± SEM.

Source data are available online for this figure.

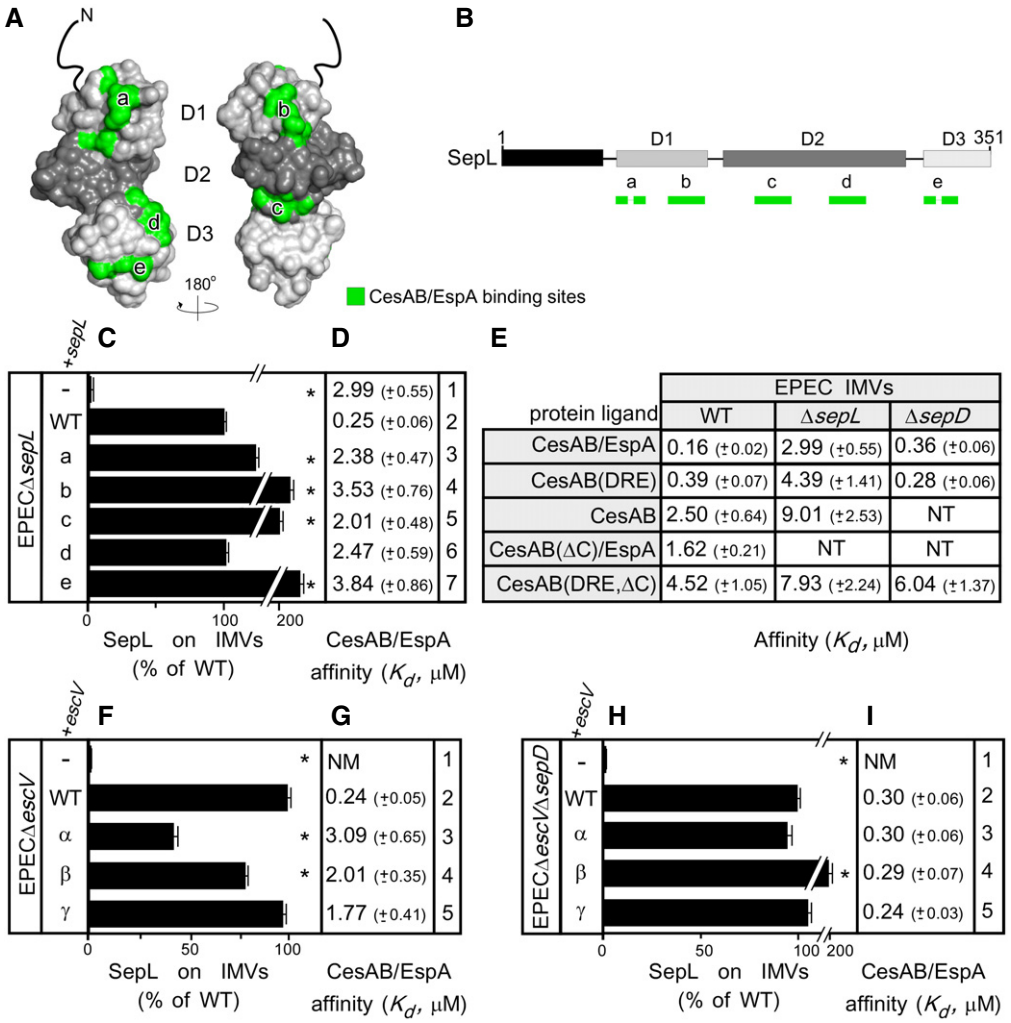

Figure 4. Requirements for CesAB/EspA targeting to SepL.

A, B The CesAB/EspA binding sites (green), as determined by peptide arrays (Fig EV4A), are indicated on the surface structure (A) or the linear map (B) of SepL.

C–I The SepL content (C, F, and H) for the indicated urea-treated IMVs (Appendix Fig S2A, J and P, respectively) was quantified (as in Fig 3D); n = 3; bar graphs represent mean values; error bars standard deviation (SD). K_ds of protein ligands (D, E, G, and I) for urea-treated EPEC IMVs (as indicated; as in Figs 2E and EV2D); n = 6–9; mean ± SEM. Mutated sites on SepL (a–e) and EscV (α–γ) are detailed in Appendix Supplementary Materials and Methods. Significant difference with P-values < 0.05, as determined by t-test and adjusted by BH (see Materials and Methods) is indicated with an asterisk (*).

with low affinity on EPECΔ*sepL* IMVs (4.39 μM), arguing that CesAB is the component of the complex that is specifically recognized by SepL.

Deletion of the CesAB C-tail reduced the affinity of either CesAB (ΔC)/EspA or CesAB(DRE,ΔC) for EPEC IMVs by 10-fold (Fig 4E, 1.62 and 4.52 μM, respectively), pointing out that the C-tail is a main element responsible for high-affinity binding on SepL, in agreement with the fractionation results (Fig 1C). EspA had an additional but minor contribution, directly or indirectly, to CesAB/EspA binding (Fig 4E, compare CesAB/EspA to CesAB(DRE) in wt or Δ*sepL* IMVs).

EscV controls the SepL receptor function through their physical interaction

To test whether the EscV-SepL interaction affects the receptor function of SepL, surface-exposed residues of EscV located on its SepL-binding patches (Fig 3I) were alanyl or seryl substituted on plasmid-borne *escV* (Fig EV4F; detailed in Appendix Supplementary Materials and Methods) and transformed into EPECΔ*escV* cells. IMVs were prepared, and their SepL content (Fig 4F; Appendix Fig S2J) and affinity for CesAB/EspA (Fig 4G) were determined.

Wild-type, plasmid-borne *escV* restored both the membrane association between SepL and CesAB/EspA affinity (Fig 4F and G, compare row 1 to 2). All *escV* mutants supported almost wild-type levels of membrane-associated SepL (Fig 4F, rows 3–5), presumably since SepL does not depend solely on its interaction with the C-domain of EscV to remain membrane-associated but also makes use of its N-terminal regions. Nevertheless, all derivatives lost high-affinity CesAB/EspA binding (Fig 4G, compare rows 3–5 to 2). Mutating the SepL-binding interfaces of EscV significantly affected the receptor function of wild-type SepL (Fig 4G, rows 3–5). Presumably, EscV alters the conformation of SepL, implying a dominant EscV-SepL allosteric cross-talk.

The SepL-EscV conformational cross-talk requires SepD

SepL is chaperoned by CesL and SepD [Fig EV3C, top (Younis *et al*, 2010)]. While the absence of CesL destabilized membrane-bound SepL (Fig 3D, row 5 and data not shown), that of SepD affected neither membrane association nor receptor function of SepL (Figs 3C and D, row 3, and 4E).

To test whether SepD affected the SepL-EscV interaction, we constructed the double deletion strain EPEC*ΔescVΔsepD*, transformed it with plasmids encoding *escV* mutants, prepared IMVs, and determined their SepL content and CesAB/EspA affinity. In all cases, SepL remained membrane-associated (Fig 4H; Appendix Fig S2P). Notably, removal of SepD restored high-affinity CesAB/EspA binding to the injectisomes with mutated EscVs (compare Fig 4I and G, rows 3–5) arguing that SepL and EscV were (Fig 4G), but no longer are (Fig 4I), in conformational cross-talk.

Our experiments suggest that by binding to SepL (O'Connell *et al*, 2004), SepD establishes the SepL-EscV conformational cross-talk that allows EscV to control SepL receptor function (Fig 4G and I).

SepL and SepD establish a translocator/effector affinity switch on the injectisome

Given that the SepL-EscV physical interaction determines CesAB/EspA targeting to SepL (Fig 3J), while SepD controls the SepL-EscV cross-talk, we wondered whether the same mechanism regulates switching from translocators to effectors (O'Connell *et al*, 2004; Deng *et al*, 2005). To test this, we co-purified a chaperone/effector pair, CesT/Tir [*t*ranslocated *i*ntimin *r*eceptor (Kenny *et al*, 1997)] (Fig EV3C, bottom), and determined its affinity (K_d) for various IMVs.

Wild-type EPEC IMVs bind CesAB/EspA with high and CesT/Tir with low affinity (Fig 5A, 0.16 and 2.23 μM, respectively). CesT alone exhibited twofold lower affinity (4.45 μM). Therefore, Tir binding enhanced the affinity of CesT for the translocase (Fig 5A), but not as drastically as EspA did for CesAB (Fig 4E). While EPEC*ΔsepL* IMVs lost their high affinity for CesAB/EspA, they "gained" high affinity for CesT/Tir (Fig 5A, 2.99 and 0.38 μM, respectively). SepL seems to be an affinity switch not only for translocator but also for effector complexes: positive for translocators and negative for effectors. EPEC*escV(ΔCD)* IMVs did not exhibit any affinity for CesT/Tir (Fig 5A), arguing that EscV is the primary receptor for the chaperone/effector pair.

EPEC*ΔsepD* IMVs exhibited as high affinity for CesT/Tir as for CesAB/EspA (Fig 5A, 0.26 and 0.36 μM, respectively), demonstrating that once the SepL-EscV cross-talk is disrupted, SepL cannot act anymore as a repressor of CesT/Tir binding, while it fully retains its function as a translocator receptor.

Are the SepL and the CesT/Tir interaction sites on EscV common? To address this, we generated an EPEC*ΔsepLΔescV* strain and transformed it with wild-type *escV* or derivative plasmids carrying mutations on one of the three EscV binding sites for SepL (Fig 3I). IMVs were prepared and K_ds for CesT/Tir determined. Binding of CesT/Tir (Fig 5B) was compromised, particularly for site γ, suggesting these may be universal receptor sites on the translocase.

Our results demonstrated that a single mechanism regulates targeting of both T3S translocators and effectors (Fig 5C). SepD

A

Affinity (K_d, μM)

protein ligand	EPEC IMVs			
	WT	Δ*sepL*	Δ*sepD*	*escV(ΔCD)*
CesT/Tir	2.23 (±0.82)	0.38 (±0.08)	0.26 (±0.06)	NM
CesT	4.45 (±1.07)	0.55 (±0.11)	NT	NT
CesAB/EspA	0.16 (±0.02)	2.99 (±0.82)	0.36 (±0.06)	NM

B

protein ligand	EPEC*ΔescVΔsepL* + *escV* IMVs			
	WT	α	β	γ
CesT/Tir	0.42 (±0.08)	0.63 (±0.16)	1.03 (±0.22)	2.18 (±0.76)

C

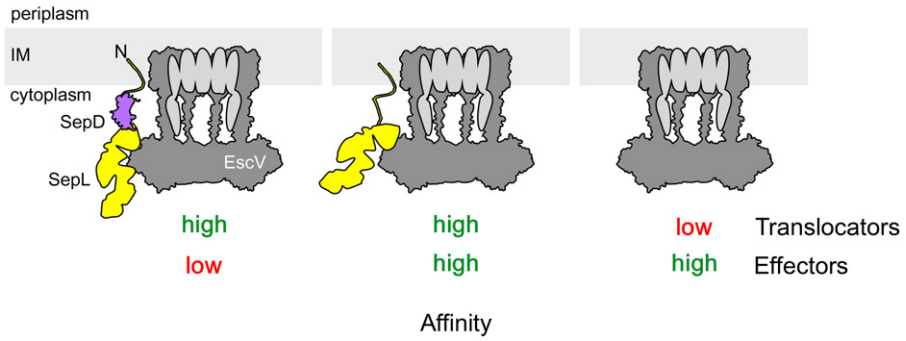

Figure 5. SepL acts as an affinity switch between translocators and effectors.

A, B K_ds of protein ligands for urea-treated EPEC IMVs (as indicated); n = 9; mean ± SEM.

C Schematic representation of the affinity switch between translocators/effectors.

binding to SepL establishes SepL-EscV conformational cross-talk that ensures translocator targeting, while repressing effector targeting (left). SepD release disrupts this cross-talk, thus leading to non-selective targeting: translocators and effectors bind to the injectisome equally well (middle). Release of the translocator receptor SepL leads to exclusive effector targeting (right).

Targeting is an essential, early step of secretion/infection

To test whether the targeting mechanism that was revealed by the *in vitro* experiments is directly related to the secretion and infection processes *in vivo*, we monitored secretion of EspA in the medium of bacterial cultures (Fig 6A, C, E, G, and I) and infection of HeLa cells by the same bacterial strains (Fig 6B, D, F, H, and J).

Bacteria devoid of CesAB, neither secreted EspA nor formed actin pedestals on HeLa cells (Fig 6A and B, compare row 2 to 1; Fig EV5I and J). Wild-type *cesAB* expressed *in trans* restored both phenotypes (Fig 6A and B, compare row 3 to 1; Fig EV5F lanes 2–4, and K). On the contrary, *cesAB* derivatives with mutated C-tails that exhibited targeting defects [i.e., *cesAB*(Δ*C*) and *cesAB*(6A), a mutant in which the six positive charges of the C-tail were substituted by alanines; data not shown] complemented neither phenotype (Fig 6A and B, rows 4 and 5; Fig EV5F, L and M). These defects were not corrected even after *CesAB*(ΔC)*/espA* were over-synthesized, several-fold over their K_d (Fig 6A and B, row 6; Fig EV5A–C), demonstrating a role of the C-tail not only in the targeting but also in the downstream secretion step.

In agreement with these results, cells devoid of the CesAB/EspA-targeting receptor SepL show no EspA secretion or HeLa infection even under conditions where CesAB/EspA was over-expressed (Fig 6C and D; Fig EV5C–E and N). *In trans* expression of wild-type *sepL* restored these defects (Fig 6E and F, row 1; Appendix Fig S2A, lane 2, top panel; Appendix Fig S2B and C). In contrast, under identical conditions, *sepL* derivatives with defective receptor sites for CesAB/EspA (Fig 4D) exhibited defects in either EspA secretion or HeLa cell infection (Fig 6E and F, rows 2–6; Appendix Fig S2A and D–I).

Moreover, mutations on *escV* that affected targeting of both CesAB/EspA (Fig 4G) and CesT/Tir (Fig 5B) practically abolished secretion of EspA as well as that of Tir (Fig 6G; Appendix Fig S2J; Fig EV5G) and infection of HeLa cells (Fig 6H; Appendix Fig S2K–O).

Clearly, targeting is an essential, early step of T3SS secretion/infection. *In vitro* targeting defects are directly correlated with compromised *in vivo* secretion and infection.

Affinity switching in T3S targeting underlies substrate secretion switching

SepD controls the SepL-EscV conformational cross-talk underlying the receptor function of SepL. To test whether this is coupled to secretion, we examined the secretion of EspA and Tir in the medium of bacterial cultures (Fig 6I, as indicated; Fig EV5H) of wild-type (row 1), Δ*sepL* (row 2), Δ*sepD* (row 3), and Δ*cesL* (row 4) EPEC cells. None of these deletion strains grown in bacterial cultures secreted translocators (i.e., EspA, EspB, and EspD; Fig EV5H). All three had switched to effector secretion (e.g., Tir, NleA; Fig EV5H), as anticipated by the *in vitro* targeting results (Fig 5A and data not shown). However, in the absence of translocator-built channels, none of them infected HeLa cells (Fig 6J; Appendix Fig S1F–H).

We concluded that SepD couples the translocator receptor function of SepL to the biochemically distinct, succeeding, secretion step (Fig 6K, left). This coupling mechanism most likely also involves chaperone elements, such as the CesAB C-tail. Release of SepD alters the SepL-EscV interaction, thus uncoupling the translocator receptor function of SepL from that of secretion (middle). This new state allows now effector binding to EscV and secretion. SepL release may consolidate switching of the injectisome to dedicated binding and secretion of late substrates (right).

Discussion

How exported proteins are targeted to the injectisome of T3SS-harboring bacteria, how the translocase is activated for secretion, and how the hierarchy of the appropriate exported substrate is imposed have remained elusive. The absence of *in vitro* systems has hindered dissection of the molecular mechanism. Here, we present the first *in vitro* reconstitution of T3S targeting that allowed us to determine the order of events, quantify binding interactions, dissect receptor functions from contribution to secretion, and determine the molecular basis of translocator-effector switching.

CesAB targets EspA to the membrane mainly via its dynamic and unstructured C-tail (Fig 1B and C). In inactive CesAB dimers, the C-tail is solvent-accessible but presumably unavailable for high-affinity targeting. EspA binding to CesAB relieves this auto-inhibition and conformationally primes CesAB for two events: electrostatic docking of the C-tail on the membrane-associated SepL (Fig 4A, D, and E; Fig EV2A) and molecular recognition of the N-core by the EscN ATPase (Chen *et al*, 2013). Since chaperone/substrate docking on SepL does not require EscN (Fig 3C, lane 6), CesAB/EspA association with SepL precedes that with EscN. This simple mechanism couples membrane targeting to the next, ATPase-catalyzed step, generally believed to cause dissociation of the exported protein from the chaperone and initiate its translocation (Akeda & Galan, 2005; Chen *et al*, 2013).

That SepL acts as a CesAB receptor was both unexpected and remarkable. SepL and homologous gatekeepers (e.g., MxiC, CopN, YopN/TyeA) are considered as exported, effector-like proteins with N-terminal signal peptides (Fields & Hackstadt, 2000; Botteaux *et al*, 2009; Younis *et al*, 2010; Amer *et al*, 2016). However, if and how their own export relates to that of translocators or effectors is unclear (Roehrich *et al*, 2017). Gatekeepers might recognize specific sequences that lie downstream of the N-terminal signal sequences of translocators, for example, in EspB (Deng *et al*, 2015; Roehrich *et al*, 2017). We anticipate that the novel receptor role revealed here and analyzed in detail for CesAB might be universal for translocator chaperones, even those structurally distinct from CesAB [e.g., the CesD and CesD2 class III chaperones of EspB and D (Wainwright & Kaper, 1998; Neves *et al*, 2003)]. This would be in agreement with, structures of gatekeepers co-complexed with chaperone homologues (Archuleta & Spiller, 2014), pull-down assays (Kubori & Galan, 2002; Silva-Herzog *et al*, 2011), and the abolished secretion of all translocators in SepL, SepD, and CesL mutants (Fig EV5H; Wang *et al*, 2008; Younis *et al*, 2010; Deng *et al*, 2015). In this capacity,

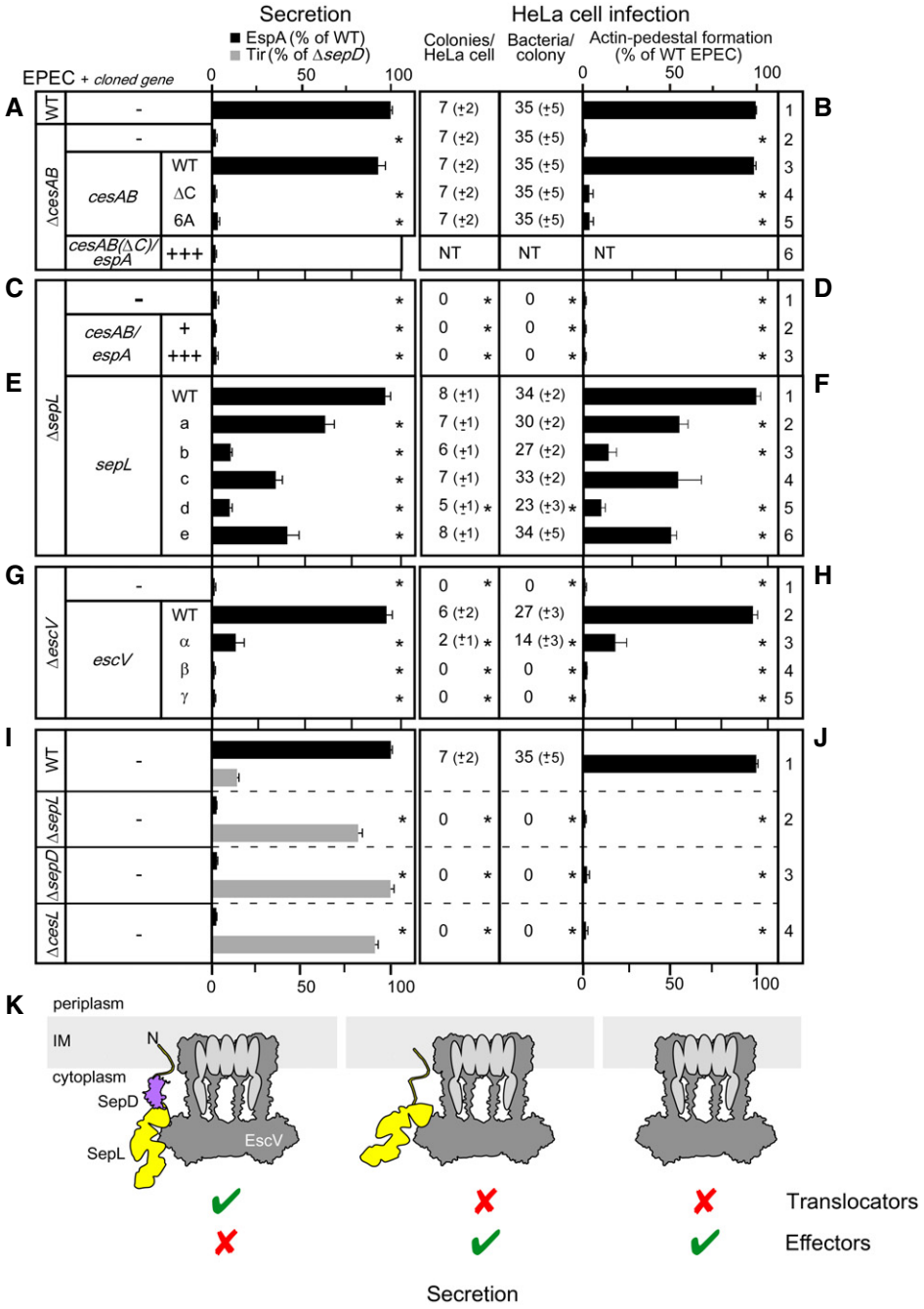

Figure 6. Affinity switching in T3S targeting underlies secretion switching.

A–J EspA and Tir secretion (A, C, E, G, and I) from various EPEC strains carrying, or not, plasmids (as indicated; Appendix Fig S2A and J; Fig EV5C, F, and H) was quantified (as in Fig 3B); n = 3; bar graphs represent mean values; error bars standard deviation (SD). +, chromosomal level expression; +++, overexpression. The HeLa cell infection by the indicated EPEC strains (B, D, F, H, and J) was quantified for: colonies formed/HeLa cell, bacteria found/colony and actin pedestal formation (for representative micrographs, see Appendix Fig S1F–H; Fig S2B–I and K–O; Fig EV5I–N; ~100 HeLa cells/experiment were examined). Results are presented as % of wild type, with error bars. n = 3; bar graphs represent mean values; error bars standard deviation (SD). Significant difference with P-values < 0.05, as determined by t-test and adjusted by BH (see Materials and Methods) is indicated with an asterisk (*).

K Schematic representation of the secretion switch between translocators/effectors.

SepL may act indeed as an early pseudo-effector (Younis *et al*, 2010), that occupies EscV, switches it to preferentially accepting translocators and blocks binding of all other effectors.

While EspA-activated CesAB alone, specifically recognizes SepL with high affinity (Figs 4E and EV4A and B), EspA marginally enhances this binding (~2- to 3-fold). This effect could be mediated

indirectly, for example, by EspA optimizing the conformation of CesAB for SepL docking, or directly, for example, through recognition of EspA by EscV. Such interaction would also rationalize the low-affinity binding component of CesAB/EspA for EscV (i.e., Δ*sepL*, Fig 3J). In the flagellum system, the C-terminal region of substrate loaded-chaperones targets the chaperone/secretory protein complex to the C-domain of the EscV homologue, FlhA with higher affinity than the chaperone alone (Bange *et al*, 2010; Minamino *et al*, 2012; Kinoshita *et al*, 2013, 2016; Furukawa *et al*, 2016). Defining the structural basis of such interactions with EscV is a major challenge due to its multimeric and membrane-embedded nature. Targeting modes of T3S chaperone/exported protein pairs may be variable, but EscV is unique, and hence, entrance and movement through its 5-nm-wide C-domain ante-chamber and the transmembrane EscRST channel around which the nonamer seems assembled (Abrusci *et al*, 2013; Hu *et al*, 2017) are expected to be universally conserved for all T3S exported proteins (early, middle, or late). Attesting to this, mutations on the SepL-binding sites on EscV severely compromised secretion of Tir (Fig EV5G). Analogous promiscuity is seen in the universal Sec system where the single SecA receptor recognizes the 505 secreted proteins of *E. coli* K12 on two adjacent sites (Chatzi *et al*, 2017; Sardis *et al*, 2017).

SepL participates in multiple interactions (i.e., association with membranes, with EscV, with three different translocator chaperones, with its own two chaperones) and is flexible enough to become secreted through the translocase. These features hampered the use of internal SepL mutations to biochemically dissect its receptor function from its downstream role on EscV activation/EspA secretion. However, dissection was achieved by removing SepD (Figs 4E, H and I, and 5A). This provided important mechanistic insight: Targeting can be completely dissected from secretion reactions. Although limited trypsinolysis demonstrated that SepL harbors a structured 3-domain core (Fig 3G, lanes 3–6), several observations suggest that SepL is conformationally flexible: the multiplicity of its ligands and topology, its protease susceptibility while membrane-bound (Fig 3G, lanes 10–12) contrasts the 3-domain core stability, while in the soluble state (lanes 2–6), its aggregation propensity in the absence of its chaperones (Deng *et al*, 2005; Younis *et al*, 2010; Burkinshaw *et al*, 2015), the multiple conformational states seen crystallographically (Burkinshaw *et al*, 2015) and the *Yersinia* homologue being assembled from two distinct polypeptides (Iriarte *et al*, 1998). We anticipate that SepD, the CesAB C-tail, and EscV exploit these dynamics to couple SepL receptor function to EspA secretion through EscV (Figs 4E and 6). SepD might have additional, direct roles in the secretion process and, as with other late T3SS chaperones, may directly bind to EscV. These possibilities remain to be explored.

Flux of the hundreds of house-keeping exported proteins to the bacterial cell envelope that commonly follow the Sec pathway, need not be inter-dependent, may be largely under transcriptional control and may be fine-tuned by internal conformational optimization of the secretory molecules (De Geyter *et al*, 2016; Sardis *et al*, 2017). In contrast, a hallmark of T3S is its strict secretion hierarchy. This has been imposed because a third of the injectisome components and regulators are themselves T3S substrates that can only be assembled in a defined order, as the machine is self-built and because its released effectors need to attack host processes in an orchestrated manner (Buttner, 2012; Portaliou *et al*, 2016; Deng *et al*, 2017). SepL and SepD determine translocator to effector switching as they repress the affinity of EscV for chaperone-effector

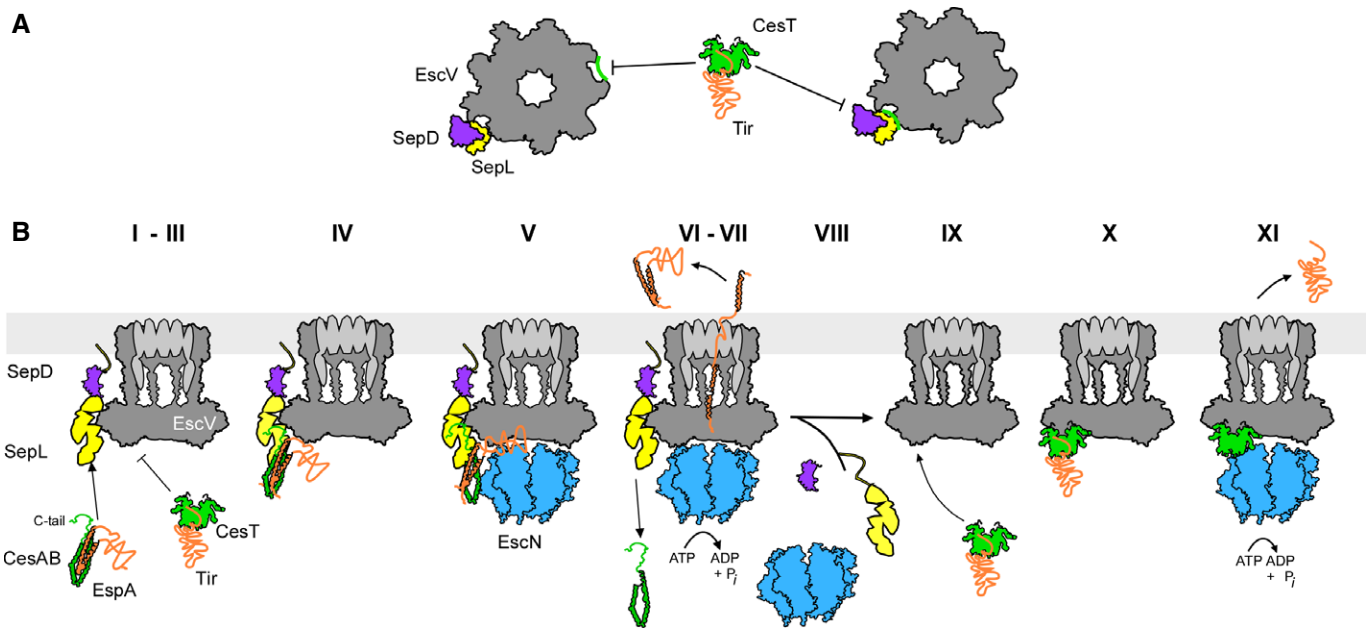

Figure 7. Working model of T3S targeting and translocator-effector switching.

A Allosteric (left) and occlusion (right) models for SepL repression of CesT/Tir targeting. The EscV nonameric ring (dark gray) is in top down view.

B Step-wise dissection of translocator/effector secretion through the T3SS (see text for details). Green: CesAB, CesT; orange: EspA, Tir; dark gray: EscV; yellow: SepL; magenta: SepD; blue: EscN. CesL (not shown) probably forms heterodimers with SepD. The EscV nonameric ring (dark gray) is in side view.

complexes until translocator secretion is complete. This mechanism provides for the first-time molecular understanding of how effector molecules are prevented from being exported, while they have been already synthesized and diffusing in the cytoplasm (Deng *et al*, 2005). The structural basis of this repression is not currently known but will undoubtedly be determined by the conformational states of the nonameric translocase component EscV. We consider two likely modes: In an "allosteric regulation" model, SepL/SepD acquire a particular conformation and bind externally to an EscV intraprotomeric groove. This causes long range allosteric changes that affect EscV conformation along all nine subunits and alter a CesT/Tir receptor site located elsewhere on the ring (Fig 7A, left). The finding that sub-stoichiometric amounts of SepL are sufficient for CesAB/EspA binding (Fig 3D, lanes 7 and 8) is consistent with this model. In a "receptor occlusion" model (Fig 7A, right), SepL and CesT/Tir bind to overlapping surfaces on EscV. Whenever SepL is bound, access of CesT/Tir to the receptor cleft is sterically prevented. Future biochemical and structural studies will be required to resolve these possibilities.

Whichever the SepL-mediated suppression mechanism is, at some point, repression ceases and effector secretion proceeds. Given the physical SepL/EscV contact, SepL would have to detach from EscV, at least partially, to allow for effector secretion. Three possible ways to gradually empty EscV sites will be probed in future studies: (i) SepD dissociation; (ii) SepL secretion (Botteaux *et al*, 2009; Younis *et al*, 2010; Roehrich *et al*, 2017); and (iii) SepL detachment from the membrane.

Synthesis of our data and those of others allowed us to propose a working model for targeting and secretion through the T3S translocase: (i) EspA binding to the N-core of CesAB monomerizes (Chen *et al*, 2011) and activates it for membrane targeting. (ii) SepL bound to SepD/CesL diffuses to the membrane where it binds to a location adjacent to EscV and thereby (iii) represses CesT/Tir binding to EscV. (iv) CesAB/EspA bind to EscV-associated SepL mainly *via* the CesAB C-tail and N-core contacts, while EspA might also weakly associate with EscV. (v) The ATPase binds to the activated CesAB N-core (Chen *et al*, 2013) and (vi) cycles of ATP hydrolysis dissociate EspA from CesAB (Akeda & Galan, 2005) and release CesAB to the cytoplasm. (vii). Multiple cycles of ATP hydrolysis and the PMF (Andrade *et al*, 2007; Lee & Rietsch, 2015) drive secretion of EspA. (viii) The SepL/D affinity switch becomes disengaged from EscV and no longer represses CesT/Tir binding. (ix) The affinity of EscV for CesT/Tir increases, (x) CesT/Tir associate with high affinity to EscV and (xi) become secreted after re-docking of the ATPase and a repeat of the cycle described for CesAB/EspA.

The availability of an *in vitro* system for CesAB/EspA and CesT/Tir targeting paves the way for a complete functional *in vitro* reconstitution of the T3S machinery that will allow systematic dissection of all the reaction steps and testing of mechanistic predictions. Together with structural and biophysical data, this promises to provide mechanistic insight in this complex, tightly regulated protein trafficking machine.

Materials and Methods

For the complete list of strains, plasmids, mutants, primers, buffers, antibodies, immobilized peptides on peptide arrays, peptide and protein list identified by MS and HDX-MS analysis, see Appendix and Source Data.

Cell growth, induction of gene expression, *in vivo* secretion

EPEC strains were grown (DMEM; 37°C; 5 h); plasmid gene expression was induced (OD_{600} = 0.3; AHT; 2.5 ng/ml; 3 h or as indicated). Cells were harvested (5,000 *g*; 20 min; 4°C); the spent medium was TCA-precipitated (20% w/v) and resuspended in volumes adjusted according to OD_{600} (1.5 M Tris–HCl pH 8.8). An equal amount of cells or supernatant derived from equal amount of cells were analyzed on SDS–PAGE, and immuno- or Coomassie Blue-stained.

Intracellular complexes and subcellular protein localization

Bacteria were sonicated (3 h post-induction; Buffer A; ethanol-dry-ice bath; 30 s × 15 cycles). Unbroken cells were removed (5,000 *g*; 20 min; 4°C) before ultracentrifugation (300,000 *g*; 30 min; 4°C). Equal amount of cytosolic or membrane proteins was analyzed (15% SDS–PAGE; 7% Native-PAGE; 30 mA; 4°C; 15 h) and immunostained.

Limited trypsinolysis and N-terminal sequencing

Purified soluble protein (1 μg) mixed with 29 μg BSA or 1 μg of the same IMV-bound protein/30 μg of total membrane protein were incubated with trypsin (Roche; 0.5 μg/sample) before Pefabloc addition (0.01 M; Roche). Following 5.5 M urea-15% SDS–PAGE, peptides were electro-transferred onto ProBlott (Applied Biosystems; 10 mM CAPS pH 11; 10% methanol), Coomassie Blue-stained and N-terminally sequenced (Alta Bioscience; Birmingham, UK).

Purification of inverted Inner membrane vesicles

As described (Chatzi *et al*, 2017; Tsolis & Economou, 2017a); detailed in Appendix Supplementary Materials and Methods.

Flotation assays

As described (Papanikou *et al*, 2005; Karamanou *et al*, 2008) with a gradient modification (2 M loading; 30 μl 1.8 M; 75 μl 1.5 M; 20 μl 1 M sucrose in Buffer C); 7 × 25 μl fractions were collected.

Equilibrium dissociation constants (K_d)

As described (Gouridis *et al*, 2009, 2010, 2013; Karamanou *et al*, 2008); detailed in Appendix Supplementary Materials and Methods. Briefly, urea-treated IMVs (20 μg/sample) were incubated with a wide range of protein ligand concentration (0–5,000 nM) mixed with a tracer amount of [^{35}S]-labeled protein ligand (Buffer C; 4°C).

Peptide array experiments

As described (Karamanou *et al*, 2008) with three sequential blotting transfers to PVDF (30 min; 1.5 h; 1.5 h). Following immunostaining, Image Quant (GE Healthcare) was used to quantify the intensity of ligand binding-signals on peptide arrays.

Quantification of signals

Expressed or secreted, soluble or IMV-bound proteins, wherever indicated, were quantified using Western blot analysis, against a standard curve of purified protein and Image Quant software (GE). Protein amount is relative to wt control or input, present on the same gel, which represented 100%. For significance test, a two-side *t*-test was used without assuming equal variance. Calculated *P*-values were adjusted for multiple hypothesis testing error using the "Benjamini–Hochberg" (Benjamini & Hochberg, 1995) method, as previously described (Tsolis *et al*, 2016; Tsolis & Economou, 2017b).

Miscellaneous

Ni^{2+}-affinity chromatography was as per the manufacturer's instructions (Qiagen). SDS–PAGE, protein transfer to nitrocellulose, Western blot analysis was as per manufacturer's instructions (Bio-Rad instruction manual; see Appendix). GPC-MALS analysis, SecA ATPase assays, *in vitro* proPhoA translocation assays (Gouridis *et al*, 2010; Karamanou *et al*, 1999), and HeLa cell infection (Creasey *et al*, 2003) were as previously described.

Data availability

MS data are available via ProteomeXchange with identifier PXD007087.

Expanded View for this article is available online.

Acknowledgements

We thank L. Persoons and K. Lepaige for HeLa cells, P. Baatsen for EM microscopy, V. Zorzini for modeling the EscV C-Domain nonamer, S. Munck and N. Corthout for access to fluorescence microscopes and guidance, S. Carpentier for help with Mass spectrometry, M. Koukaki for plasmids, O. Tomoaki for strains. This work was supported by grants (to AE): KUL-Spa (Onderzoekstoelagen 2013; Bijzonder Onderzoeksfonds; KU Leuven); RiMembR (Vlaanderen Onderzoeksprojecten; #G0C6814N; FWO); T3RecS (#G002516N; FWO); and DIP-BiD (#AKUL/15/40–G0H2116N; Hercules/FWO) and (to SK): #G0B4915N; FWO and (to JR): R&D Pilot project-2015 [Instruct, part of the European Strategy Forum on Research Infrastructures (ESFRI) and supported by national member subscriptions], (to GF): Wellcome Trust and (to C.G.K.): NIH Grant AI094623.

Author contributions

AGP performed *in vivo* and *in vitro* assays and molecular cloning; KCT performed proteomics analysis, molecular cloning, genetic knockouts, statistical analysis, and antibody preparation; MSL and VB contributed in molecular cloning, antibody preparation, genetic knockouts, secretion and infection assays; JR performed cross-linking experiments; AT performed HDX-MS experiments; VFC, CGK, and GF contributed in training, strains, and molecular cloning; SK trained and supervised biochemical and biophysical experiments; SK and AE wrote the paper with contributions from AGP and KCT and editing from GF and CGK; AE and SK conceived and supervised the project.

Conflict of interest

The authors declare that they have no conflict of interest.

References

Abe A, de Grado M, Pfuetzner RA, Sanchez-Sanmartin C, Devinney R, Puente JL, Strynadka NC, Finlay BB (1999) Enteropathogenic *Escherichia coli* translocated intimin receptor, Tir, requires a specific chaperone for stable secretion. *Mol Microbiol* 33: 1162 – 1175

Abrusci P, Vergara-Irigaray M, Johnson S, Beeby MD, Hendrixson DR, Roversi P, Friede ME, Deane JE, Jensen GJ, Tang CM, Lea SM (2013) Architecture of the major component of the type III secretion system export apparatus. *Nat Struct Mol Biol* 20: 99 – 104

Akeda Y, Galan JE (2005) Chaperone release and unfolding of substrates in type III secretion. *Nature* 437: 911 – 915

Amer AA, Gurung JM, Costa TR, Ruuth K, Zavialov AV, Forsberg A, Francis MS (2016) YopN and TyeA hydrophobic contacts required for regulating Ysc-Yop Type III secretion activity by yersinia pseudotuberculosis. *Front Cell Infect Microbiol* 6: 66

Andrade A, Pardo JP, Espinosa N, Perez-Hernandez G, Gonzalez-Pedrajo B (2007) Enzymatic characterization of the enteropathogenic *Escherichia coli* type III secretion ATPase EscN. *Arch Biochem Biophys* 468: 121 – 127

Archuleta TL, Spiller BW (2014) A gatekeeper chaperone complex directs translocator secretion during type three secretion. *PLoS Pathog* 10: e1004498

Bange G, Kummerer N, Engel C, Bozkurt G, Wild K, Sinning I (2010) FlhA provides the adaptor for coordinated delivery of late flagella building blocks to the type III secretion system. *Proc Natl Acad Sci USA* 107: 11295 – 11300

Benjamini Y, Hochberg Y (1995) Controlling the false discovery rate: a practical and powerful approach to multiple testing. *J R Stat Soc B* 57: 289 – 300

Botteaux A, Sory MP, Biskri L, Parsot C, Allaoui A (2009) MxiC is secreted by and controls the substrate specificity of the *Shigella flexneri* type III secretion apparatus. *Mol Microbiol* 71: 449 – 460

Burkinshaw BJ, Souza SA, Strynadka NC (2015) Structural analysis of SepL, an enteropathogenic *Escherichia coli* type III secretion-system gatekeeper protein. *Acta Crystallogr F Struct Biol Commun* 71: 1300 – 1308

Buttner D (2012) Protein export according to schedule: architecture, assembly, and regulation of type III secretion systems from plant- and animal-pathogenic bacteria. *Microbiol Mol Biol Rev* 76: 262 – 310

Callister SJ, Barry RC, Adkins JN, Johnson ET, Qian WJ, Webb-Robertson BJ, Smith RD, Lipton MS (2006) Normalization approaches for removing systematic biases associated with mass spectrometry and label-free proteomics. *J Proteome Res* 5: 277 – 286

Chatzi KE, Sardis MF, Tsirigotaki A, Koukaki M, Sostaric N, Konijnenberg A, Sobott F, Kalodimos CG, Karamanou S, Economou A (2017) Preprotein mature domains contain translocase targeting signals that are essential for secretion. *J Cell Biol* 216: 1357 – 1369

Chen L, Balabanidou V, Remeta DP, Minetti CA, Portaliou AG, Economou A, Kalodimos CG (2011) Structural instability tuning as a regulatory mechanism in protein-protein interactions. *Mol Cell* 44: 734 – 744

Chen L, Ai X, Portaliou AG, Minetti CA, Remeta DP, Economou A, Kalodimos CG (2013) Substrate-activated conformational switch on chaperones encodes a targeting signal in type III secretion. *Cell Rep* 3: 709 – 715

Creasey EA, Friedberg D, Shaw RK, Umanski T, Knutton S, Rosenshine I, Frankel G (2003) CesAB is an enteropathogenic *Escherichia coli* chaperone for the type-III translocator proteins EspA and EspB. *Microbiology* 149: 3639 – 3647

De Geyter J, Tsirigotaki A, Orfanoudaki G, Zorzini V, Economou A, Karamanou S (2016) Protein folding in the cell envelope of *Escherichia coli*. *Nat Microbiol* 1: 16107

Dean P, Kenny B (2009) The effector repertoire of enteropathogenic *E. coli*: ganging up on the host cell. *Curr Opin Microbiol* 12: 101 – 109

Deng W, Li Y, Hardwidge PR, Frey EA, Pfuetzner RA, Lee S, Gruenheid S, Strynakda NC, Puente JL, Finlay BB (2005) Regulation of type III secretion hierarchy of translocators and effectors in attaching and effacing bacterial pathogens. *Infect Immun* 73: 2135 – 2146

Deng W, Yu HB, Li Y, Finlay BB (2015) SepD/SepL-dependent secretion signals of the type III secretion system translocator proteins in enteropathogenic *Escherichia coli*. *J Bacteriol* 197: 1263 – 1275

Deng W, Marshall NC, Rowland JL, McCoy JM, Worrall LJ, Santos AS, Strynadka NCJ, Finlay BB (2017) Assembly, structure, function and regulation of type III secretion systems. *Nat Rev Microbiol* 15: 323 – 337; Corrigendum: 15: 379

Dziva F, van Diemen PM, Stevens MP, Smith AJ, Wallis TS (2004) Identification of *Escherichia coli* O157: H7 genes influencing colonization of the bovine gastrointestinal tract using signature-tagged mutagenesis. *Microbiology* 150: 3631 – 3645

Elliott SJ, O'Connell CB, Koutsouris A, Brinkley C, Donnenberg MS, Hecht G, Kaper JB (2002) A gene from the locus of enterocyte effacement that is required for enteropathogenic *Escherichia coli* to increase tight-junction permeability encodes a chaperone for EspF. *Infect Immun* 70: 2271 – 2277

Fields KA, Hackstadt T (2000) Evidence for the secretion of *Chlamydia trachomatis* CopN by a type III secretion mechanism. *Mol Microbiol* 38: 1048 – 1060

Furukawa Y, Inoue Y, Sakaguchi A, Mori Y, Fukumura T, Miyata T, Namba K, Minamino T (2016) Structural stability of flagellin subunit affects the rate of flagellin export in the absence of FliS chaperone. *Mol Microbiol* 102: 405 – 416

Gauthier A, Puente JL, Finlay BB (2003) Secretin of the enteropathogenic *Escherichia coli* type III secretion system requires components of the type III apparatus for assembly and localization. *Infect Immun* 71: 3310 – 3319

Gouridis G, Karamanou S, Gelis I, Kalodimos CG, Economou A (2009) Signal peptides are allosteric activators of the protein translocase. *Nature* 462: 363 – 367

Gouridis G, Karamanou S, Koukaki M, Economou A (2010) *In vitro* assays to analyze translocation of the model secretory preprotein alkaline phosphatase. *Methods Mol Biol* 619: 157 – 172

Gouridis G, Karamanou S, Sardis MF, Scharer MA, Capitani G, Economou A (2013) Quaternary dynamics of the SecA motor drive translocase catalysis. *Mol Cell* 52: 655 – 666

Hu B, Lara-Tejero M, Kong Q, Galan JE, Liu J (2017) *In situ* molecular architecture of the salmonella type III secretion machine. *Cell* 168: 1065 – 1074.e1010

Iriarte M, Sory MP, Boland A, Boyd AP, Mills SD, Lambermont I, Cornelis GR (1998) TyeA, a protein involved in control of Yop release and in translocation of Yersinia Yop effectors. *EMBO J* 17: 1907 – 1918

Karamanou S, Vrontou E, Sianidis G, Baud C, Roos T, Kuhn A, Politou AS, Economou A (1999) A molecular switch in SecA protein couples ATP hydrolysis to protein translocation. *Mol Microbiol* 34: 1133 – 1145

Karamanou S, Bariami V, Papanikou E, Kalodimos CG, Economou A (2008) Assembly of the translocase motor onto the preprotein-conducting channel. *Mol Microbiol* 70: 311 – 322

Kenny B, DeVinney R, Stein M, Reinscheid DJ, Frey EA, Finlay BB (1997) Enteropathogenic *E. coli* (EPEC) transfers its receptor for intimate adherence into mammalian cells. *Cell* 91: 511 – 520

Kinoshita M, Hara N, Imada K, Namba K, Minamino T (2013) Interactions of bacterial flagellar chaperone-substrate complexes with FlhA contribute to co-ordinating assembly of the flagellar filament. *Mol Microbiol* 90: 1249 – 1261

Kinoshita M, Nakanishi Y, Furukawa Y, Namba K, Imada K, Minamino T (2016) Rearrangements of alpha-helical structures of FlgN chaperone control the binding affinity for its cognate substrates during flagellar type III export. *Mol Microbiol* 101: 656 – 670

Knutton S, Rosenshine I, Pallen MJ, Nisan I, Neves BC, Bain C, Wolff C, Dougan G, Frankel G (1998) A novel EspA-associated surface organelle of enteropathogenic *Escherichia coli* involved in protein translocation into epithelial cells. *EMBO J* 17: 2166 – 2176

Kubori T, Galan JE (2002) Salmonella type III secretion-associated protein InvE controls translocation of effector proteins into host cells. *J Bacteriol* 184: 4699 – 4708

Lee PC, Rietsch A (2015) Fueling type III secretion. *Trends Microbiol* 23: 296 – 300

Minamino T, Kinoshita M, Hara N, Takeuchi S, Hida A, Koya S, Glenwright H, Imada K, Aldridge PD, Namba K (2012) Interaction of a bacterial flagellar chaperone FlgN with FlhA is required for efficient export of its cognate substrates. *Mol Microbiol* 83: 775 – 788

Nadler C, Shifrin Y, Nov S, Kobi S, Rosenshine I (2006) Characterization of enteropathogenic *Escherichia coli* mutants that fail to disrupt host cell spreading and attachment to substratum. *Infect Immun* 74: 839 – 849

Neves BC, Mundy R, Petrovska L, Dougan G, Knutton S, Frankel G (2003) CesD2 of enteropathogenic *Escherichia coli* is a second chaperone for the type III secretion translocator protein EspD. *Infect Immun* 71: 2130 – 2141

O'Connell CB, Creasey EA, Knutton S, Elliott S, Crowther LJ, Luo W, Albert MJ, Kaper JB, Frankel G, Donnenberg MS (2004) SepL, a protein required for enteropathogenic *Escherichia coli* type III translocation, interacts with secretion component SepD. *Mol Microbiol* 52: 1613 – 1625

Papanastasiou M, Orfanoudaki G, Koukaki M, Kountourakis N, Sardis MF, Aivaliotis M, Karamanou S, Economou A (2013) The *Escherichia coli* peripheral inner membrane proteome. *Mol Cell Proteomics* 12: 599 – 610

Papanastasiou M, Orfanoudaki G, Kountourakis N, Koukaki M, Sardis MF, Aivaliotis M, Tsolis KC, Karamanou S, Economou A (2016) Rapid label-free quantitative analysis of the *E. coli* BL21(DE3) inner membrane proteome. *Proteomics* 16: 85 – 97

Papanikou E, Karamanou S, Baud C, Frank M, Sianidis G, Keramisanou D, Kalodimos CG, Kuhn A, Economou A (2005) Identification of the preprotein binding domain of SecA. *J Biol Chem* 280: 43209 – 43217

Parsot C (2003) The various and varying roles of specific chaperones in type III secretion systems. *Curr Opin Microbiol* 6: 7 – 14

Portaliou AG, Tsolis KC, Loos MS, Zorzini V, Economou A (2016) Type III secretion: building and operating a remarkable nanomachine. *Trends Biochem Sci* 41: 175 – 189

Roehrich AD, Bordignon E, Mode S, Shen DK, Liu X, Pain M, Murillo I, Martinez-Argudo I, Sessions RB, Blocker AJ (2017) Steps for shigella gatekeeper protein MxiC function in hierarchical type III secretion regulation. *J Biol Chem* 292: 1705 – 1723

Saijo-Hamano Y, Imada K, Minamino T, Kihara M, Shimada M, Kitao A, Namba K (2010) Structure of the cytoplasmic domain of FlhA and implication for flagellar type III protein export. *Mol Microbiol* 76: 260 – 268

Sardis MF, Tsirigotaki A, Chatzi KE, Portaliou AG, Gouridis G, Karamanou S, Economou A (2017) Preprotein conformational dynamics drive bivalent translocase docking and secretion. *Structure* 25: 1056 – 1067.e1056

Sato H, Frank DW (2011) Multi-functional characteristics of the *Pseudomonas aeruginosa* type III needle-tip protein, PcrV; comparison to orthologs in other gram-negative bacteria. *Front Microbiol* 2: 142

Schubot FD, Jackson MW, Penrose KJ, Cherry S, Tropea JE, Plano GV, Waugh DS (2005) Three-dimensional structure of a macromolecular assembly that regulates type III secretion in *Yersinia pestis*. *J Mol Biol* 346: 1147 – 1161

Silva-Herzog E, Joseph SS, Avery AK, Coba JA, Wolf K, Fields KA, Plano GV (2011) Scc1 (CP0432) and Scc4 (CP0033) function as a type III secretion chaperone for CopN of *Chlamydia pneumoniae*. *J Bacteriol* 193: 3490 – 3496

Thomas NA, Deng W, Puente JL, Frey EA, Yip CK, Strynadka NC, Finlay BB (2005) CesT is a multi-effector chaperone and recruitment factor required for the efficient type III secretion of both LEE- and non-LEE-encoded effectors of enteropathogenic *Escherichia coli*. *Mol Microbiol* 57: 1762 – 1779

Tsirigotaki A, De Geyter J, Sostaric N, Economou A, Karamanou S (2017a) Protein export through the bacterial Sec pathway. *Nat Rev Microbiol* 15: 21 – 36

Tsirigotaki A, Papanastasiou M, Trelle MB, Jørgensen TJD, Economou A (2017b) Chapter four – Analysis of translocation-competent secretory proteins by HDX-MS. In *Methods in enzymology*, Arun KS (ed), Vol. 586, pp 57 – 83. Cambridge, MA: Academic Press

Tsolis KC, Bagli E, Kanaki K, Zografou S, Carpentier S, Bei ES, Christoforidis S, Zervakis M, Murphy C, Fotsis T, Economou A (2016) Proteome changes during transition from human embryonic to vascular progenitor cells. *J Proteome Res* 15: 1995 – 2007

Tsolis KC, Economou A (2017a) Chapter two – Quantitative proteomics of the *E. coli* membranome. In *Methods in enzymology*, Arun KS (ed), Vol. 586, pp 15 – 36. Cambridge, MA: Academic Press

Tsolis KC, Economou A (2017b) Quantitative proteomics of the *E. coli* membranome. *Methods Enzymol* 586: 15 – 36

Wainwright LA, Kaper JB (1998) EspB and EspD require a specific chaperone for proper secretion from enteropathogenic *Escherichia coli*. *Mol Microbiol* 27: 1247 – 1260

Wang D, Roe AJ, McAteer S, Shipston MJ, Gally DL (2008) Hierarchal type III secretion of translocators and effectors from *Escherichia coli* O157:H7 requires the carboxy terminus of SepL that binds to Tir. *Mol Microbiol* 69: 1499 – 1512

Wilharm G, Dittmann S, Schmid A, Heesemann J (2007) On the role of specific chaperones, the specific ATPase, and the proton motive force in type III secretion. *Int J Med Microbiol* 297: 27 – 36

Yip CK, Finlay BB, Strynadka NC (2005) Structural characterization of a type III secretion system filament protein in complex with its chaperone. *Nat Struct Mol Biol* 12: 75 – 81

Younis R, Bingle LE, Rollauer S, Munera D, Busby SJ, Johnson S, Deane JE, Lea SM, Frankel G, Pallen MJ (2010) SepL resembles an aberrant effector in binding to a class 1 type III secretion chaperone and carrying an N-terminal secretion signal. *J Bacteriol* 192: 6093 – 6098